Available online at www.sciencedirect.com
ScienceDirect
Journal of Power Sources 167 (2007) 206–211
JOURNAL OF POWER SOURCES
www.elsevier.com/locate/jpowsour

Short communication

Fabrication of CuO film with network-like architectures through solution-immersion and their application in lithium ion batteries

Hongbo Wang [a], Qinmin Pan [a,*], Jianwei Zhao [a,b], Geping Yin [a], Pengjian Zuo [a]

[a] *Department of Applied Chemistry, Harbin Institute of Technology, Harbin 150001, PR China*
[b] *School of Chemistry and Chemical Engineering, Nanjing University, Nanjing 210008, PR China*

Received 10 January 2007; received in revised form 5 February 2007; accepted 6 February 2007
Available online 17 February 2007

Abstract

A novel CuO negative electrode with network-like architectures was fabricated on copper substrate by a simple solution-immersion step and subsequent heat treatment, which avoids the use of binder and conducting agent that necessary to the conventional electrode-preparation process. The as-prepared CuO electrodes exhibit not only high reversible capacity but also long cycling life, high rate capability in Li ion batteries. The result of this approach creates a new and attractive negative electrode with good electrochemical performance, which is simple, mild conditions, low cost, and easy control. It also opens a pathway for the application of other nanostructured materials of transition metal oxides in lithium ion batteries.

Keywords: CuO negative electrode; Network-like architecture; Solution immersion

1. Introduction

Lithium-ion batteries are widely used in portable electronics and electric vehicles due to their high energy density, long cycle life, and no memory effect. Graphitic carbon such as mesocarbon microbeads (MCMB), natural graphite is the conventional electrode materials used in lithium ion batteries [1–3]. However, limited capacity and poor rate performance of carbonaceous electrodes had stimulated researchers to explore alternative electrode materials with high capacity and good rate capability [4,5]. Fortunately, nanomaterials of transition-metal oxides confer them these desirable properties and make them valuable choice for material chemists [6–8].

Recently, nanoscale CuO with different dimensions and morphologies had been exploited for lithium ion electrode materials [9,10], and they exhibited much higher capacity than graphite. However, such a high capacity can only be achieved with the help of additives such as electronic conducting agent (often carbon black) and polymer binder, in which mixtures of CuO and electronic conducting agent were embedded in polymer binder [11]. As a result, the kinetic process of this complex electrode, such as efficient transport for both electrons and lithium ions, is limited by polymer binder. Moreover, the electrochemical performance of the electrode is strongly dependent on fabrication procedures [12,13].

Recently, many efforts have been devoted to the fabrication of one-dimensional CuO nanomaterials such as nanowires [14,15], nanoribbons [16,17], nanoneedles [18], nanofibers [19,20], nanorods [21], and nanotubes [22] on copper substrates owing to their unique structures, intriguing properties, and potential applications. Nevertheless, these nanostructured CuO films have rarely been investigated as electrode of lithium ion batteries.

Inspired by this finding, we present here a new CuO-based negative electrode for lithium ion batteries, in which CuO nanofibers with network-like architectures directly grow on copper substrate through a simple solution-immersion step and subsequent heat treatment at low temperature. The first advantage of this electrode lies in that it avoids the tedious fabrication procedures of conventional electrodes (such as the use of polymeric binder and conducting agent). This change allows not only better electric contact between the current collector and active materials but also high energy density of the electrode. Moreover, the nanostructures of the CuO films can be controlled by immersion conditions. As a result, fast transport of lithium ions and rapid electronic kinetics are possible in the resulted CuO

* Corresponding author. Tel.: +86 451 86413721; fax: +86 451 86414661.
E-mail address: panqm@hit.edu.cn (Q. Pan).

0378-7753/$ – see front matter © 2007 Elsevier B.V. All rights reserved.
doi:10.1016/j.jpowsour.2007.02.008

electrodes. In this study, we report that this new carbon-free electrode shows high reversible capacity, good rate performance and long cycling life, which is an attractive electrode in lithium ion batteries.

2. Experimental

The construction of CuO nanofibers on a copper surface was carried out by a simple chemical route involving an oxidation–dehydration process [23], as indicated below. First, copper plates (2 cm × 2 cm) were washed with 1.0 M HCl aqueous solution for 15 min and subsequently with deionized water to remove impurities. The washed copper plates were immediately immersed into 20 ml of 0.25 M NaOH aqueous solution containing 9 mM (50 mg) $K_2S_2O_8$ and 17 mM (0.1 g) sodium dodecylsulfate (SDS) at room temperature for different duration time. After reaction, the copper plates were taken out from the solution and rinsed with deionized water and dried in air. Then the copper plates were heated at 120 °C for 1 h and at 180 °C for another 2 h under N_2 atmosphere. After the furnace cooled to room temperature, copper foils with black film on their surface was obtained.

The obtained CuO films were cut into 1 cm^2 circle plates as the negative electrodes, then dried in vacuum and weighed. Lithium foil was used as the counter electrode. The electrolyte solutions were 1.0 M $LiPF_6$ in EC/DMC (1:1 by volume). Coin cells were assembled in glovebox under argon atmosphere. The electrochemical performance of the CuO electrodes were evaluated by galvanostatic discharge/charge measurement using a computer-controlled battery tester between 0.010 and 3.0 V. Cyclic voltammograms (CVs) were recorded on potentiostat CHI 604 at a scan rate of 0.5 mV s^{-1}. All the potentials indicated here were refereed to the Li/Li^+ electrode potential.

The X-ray diffraction (XRD) analysis was carried out using Philips PW-1830. Scanning electron microscope (SEM, S-4700, Hitachi) was employed to investigate surface morphology of the CuO films.

2.1. Determination of the mass of active materials CuO

Before cell-assembly, the obtained CuO films were dried in vacuum and weighed. After discharge–charge test, the cells were disassembled and the CuO electrodes were peeled, then the electrodes were put into 1.0 M HCl aqueous solution to remove the active CuO. Subsequently, the copper foils were washed in water and acetone successively. After dried in vacuum, the resulted copper foils were weighed. The weight difference of the CuO

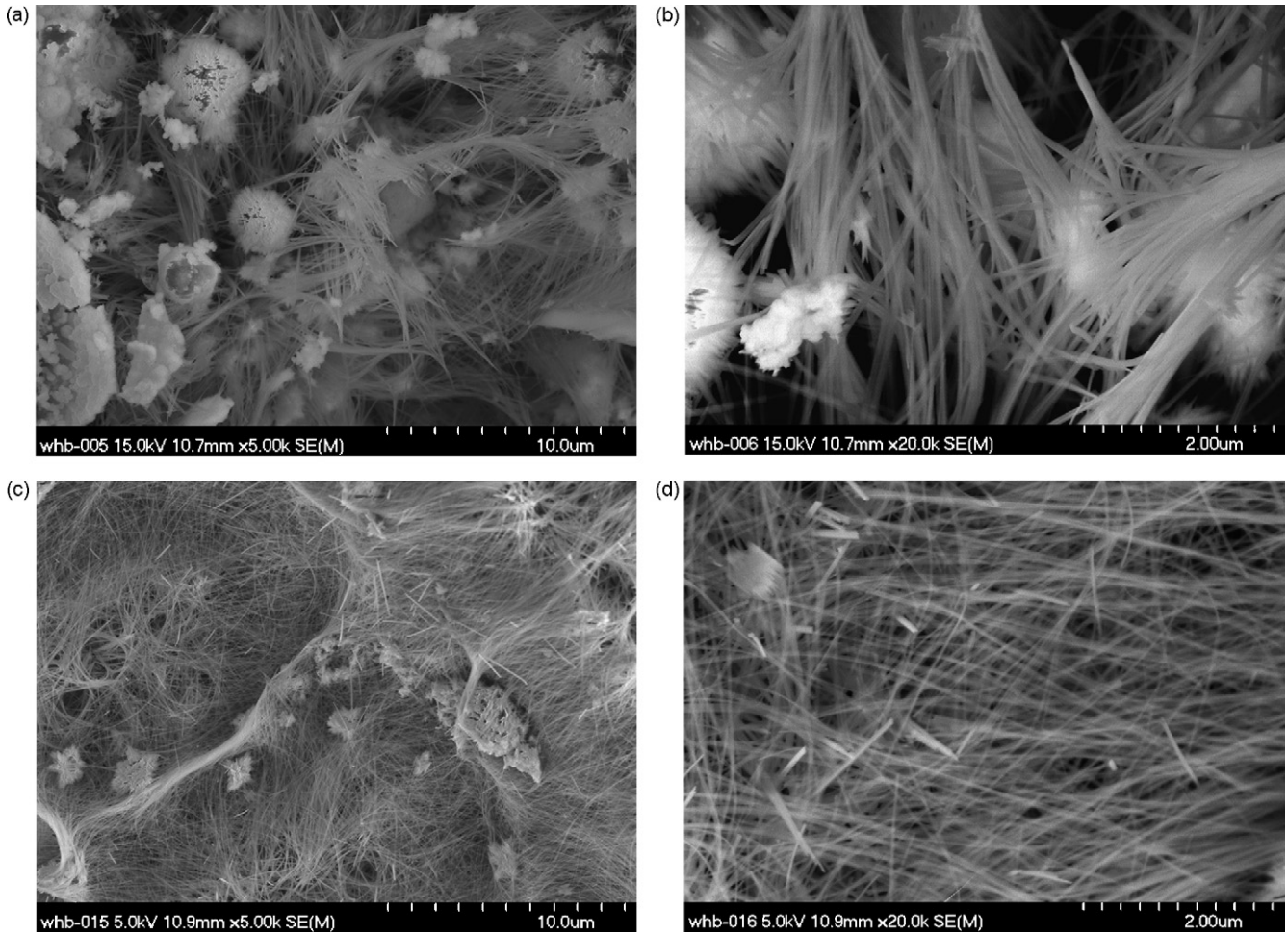

Fig. 1. Scanning electron microscopy images of the copper foils immersion in 0.25 M NaOH containing 17 mM SDS and 9 mM $K_2S_2O_8$ for (a and b) 12 h; (c and d) 24 h. (b and c) are images at higher magnifications.

films before and after washing treatment is considered to the mass of active materials CuO.

3. Results and discussion

The surface morphology of the copper foil after immersion process was investigated by scanning electron microscope, as shown in Fig. 1. We can see clearly that nanofibers with network-like architectures are observed on the copper surface. The image at higher magnifications exhibits that the nanofibers, with a length of few micrometers and a diameter of few tens nanometers, interweave into network-like architectures. Dependence of the surface morphology on immersion time was studied to gain insight into the formation process of nanofibers. Only a few nanofibers are observed on the copper surface at the beginning of solution-immersion. Upon increasing the immersion time (e.g.

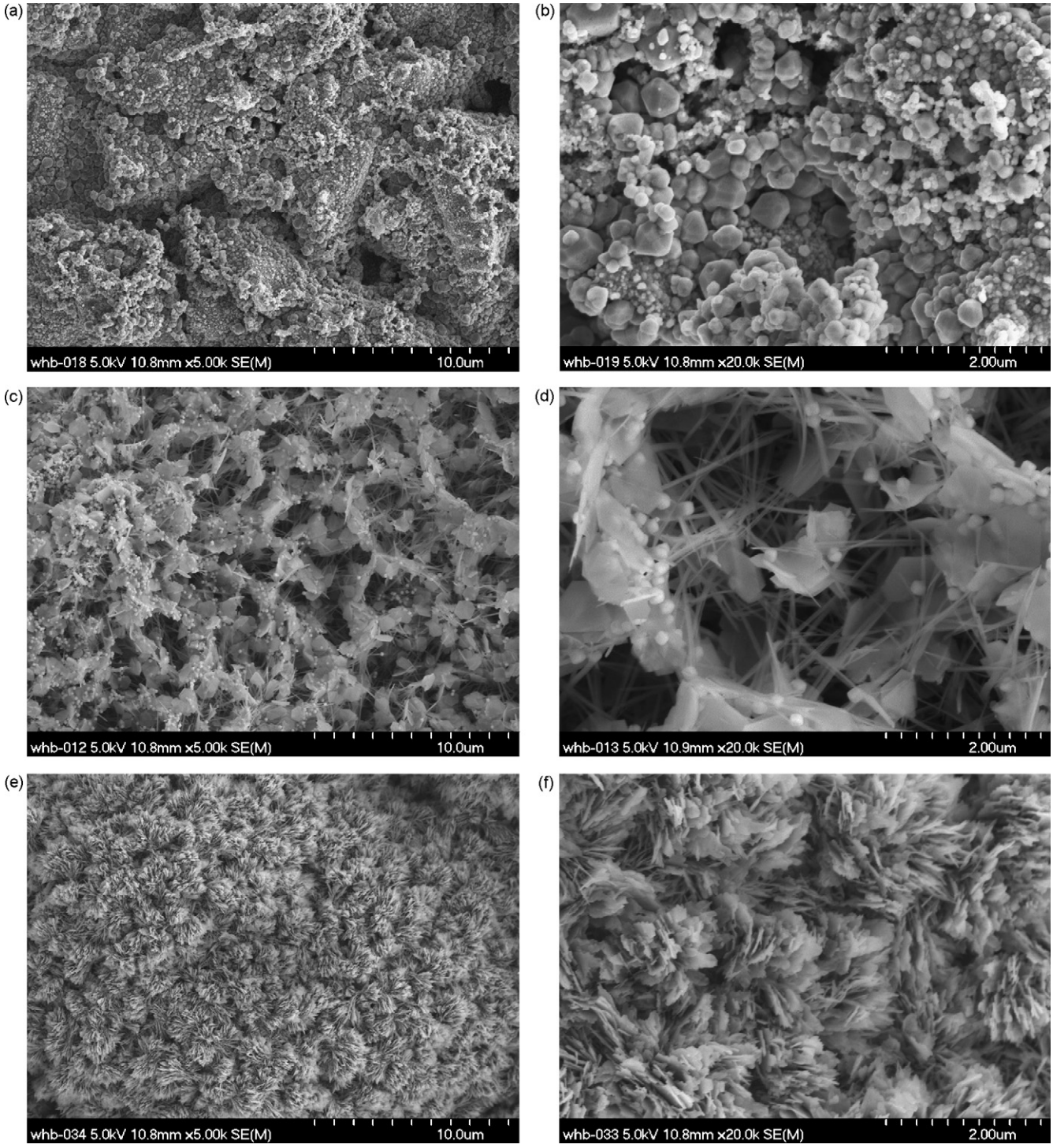

Fig. 2. Scanning electron microscopy images of the copper foils after immersion in (a and b) 0.25 M NaOH; (c and d) 0.25 M NaOH and 17 mM SDS; (e and f) 0.25 M NaOH and 9 mM $K_2S_2O_8$ for 24 h.

12 h), the surface coverage of nanofibers becomes denser (Fig. 1a and b). Then, a continuous and compact film of interwoven nanofibers distributes on the copper surface when the immersion time closes to 24 h (Fig. 1c and d).

Control experiments reveal that appropriate concentrations of sodium dodecylsulfate (SDS) and potassium persulfate ($K_2S_2O_8$) have a great influence on the morphologies of the copper surface after immersion step. In 0.25 M NaOH solution free of $K_2S_2O_8$, a large number of aggregates can be observed on the copper surface but they do not show network-like architectures, as shown in Fig. 2a–d, suggesting $K_2S_2O_8$ plays an important role in the growth of the nanofibers. Moreover, we also find that in 0.25 M NaOH/9 mM $K_2S_2O_8$ solutions without SDS, no nanofiber but rather flowerlike aggregates cover the copper surface, as illustrated in Fig. 2e and f.

To investigate the effect of heat treatment on the final surface morphology of copper samples, SEM images of a copper foil after heat treatment at 180 °C are displayed in Fig. 3. Compared with the images in Fig. 1, the copper sample after heat treatment exhibits the same network-like morphology as untreated ones. Here, we can conclude that heat treatment at low temperature of 180 °C can avoid the collapse of the fiber morphology.

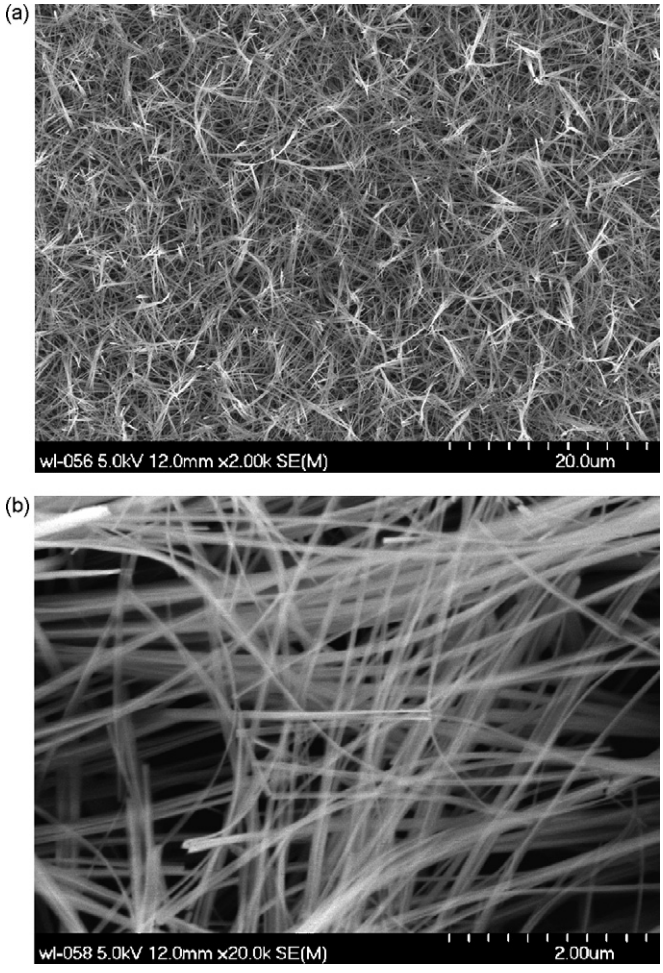

Fig. 3. Scanning electron microscopy images of the copper surface after immersion for 24 h and subsequent heat treatment at 180 °C.

The composition of the resulted sample prepared at 180 °C was examined by XRD, as shown in Fig. 4. For comparison, a XRD pattern of the Cu foil with a cubic-phase was also included. All peaks in the pattern are consistent with the JCPDS (5-0661) data of the CuO with a monoclinic phase. No peak ascribed to $Cu(OH)_2$ or Cu_2O is detected in Fig. 4b, except those marked with an asterisk from the copper substrate. Based on the XRD patterns together with the SEM images in Fig. 3, CuO nanofibers with network-like architectures were fabricated on copper surface by a simple solution-immersion step and subsequent heat treatment.

Electrochemical behaviors of the CuO negative electrode were evaluated by cyclic voltammetry and galvanostatic discharge–charge measurements. Cyclic voltammograms of the CuO electrodes at a scan rate of 0.5 mV s^{-1} are depicted in Fig. 5a. In the first scan, three cathodic peaks are observed at 1.62, 1.00 and 0.49 V, respectively; on the contrary, only one anodic peak with a small shoulder is located near 2.58 V. Generally, the cathodic peak at 1.62 V can be attributed to the reduction of O_2 and/or H_2O that are adsorbed on the CuO surface [24]. Another two cathodic peaks at 1.00 V and 0.49 V are related to the diffusion of Li ions into the CuO crystallites with the formation of the intercalated compound Li_xCuO [25,26]. Clearly, the anodic peak at 2.58 V is ascribed to lithium extraction from the crystal lattice of CuO [27]. During the second cycle, the intensities of the peaks decrease. Meanwhile, the potentials of the cathodic peaks shift to 2.21, 1.17 and 0.60 V, respectively. After initial two cycles, there is no substantial change in the peak potentials and curve shapes. The variations in intensity and shape of the peaks at the first and second scans clearly indicate the presence of irreversible capacity loss.

The initial five discharge–charge curves of the CuO electrode at a current density of 0.15 mA cm^{-2} are illustrated in Fig. 5b. There are three potential slopes at 2.1–1.8 V, 1.3–1.1 V, and 0.9–0.01 V during the first discharge process; the potential ranges of these slopes are well consistent with that of the cathodic peaks in CVs. During the second discharge process, the first potential slope (2.1–1.8 V) is narrowed and shifts slightly upward, accompanied by a decrease in the discharge capacity. The change in the potential range and discharge capacity during the first and second discharges are consistent with the observation in CVs. The initial discharge capacity of the obtained CuO electrode is about 970 mAh g^{-1}, which is larger than the theoretical capacity of 674 mAh g^{-1} based on a maximum uptake of 2Li/CuO. The large excesses capacity can be attributed to the decomposition of the electrolyte and subsequent formation of the passive film on the CuO surface that occurs in the low potential region [28,29]. Moreover, the reduction of the adsorbed impurities on the CuO surface, the initial formation of lithium oxide [30], and the presence of some residual OH^- groups in the active CuO [31] are also responsible for the additional discharge capacity.

Cycling performance of the CuO electrode at a current density of 0.2 mA cm^{-2} is shown in Fig. 6. It can be found that the electrode exhibit a high capacity and a slow capacity fading. A stable reversible capacity of 560 mAh g^{-1} can be achieved after the second cycle, and the CuO electrode still keeps its

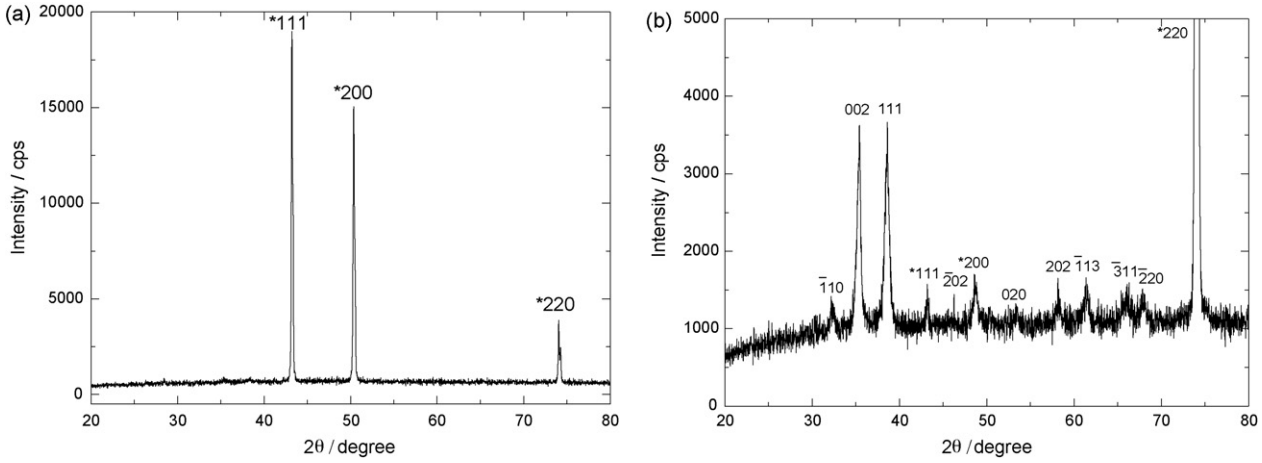

Fig. 4. XRD patterns of the (a) Cu foil and (b) CuO nanofibers on the copper surface.

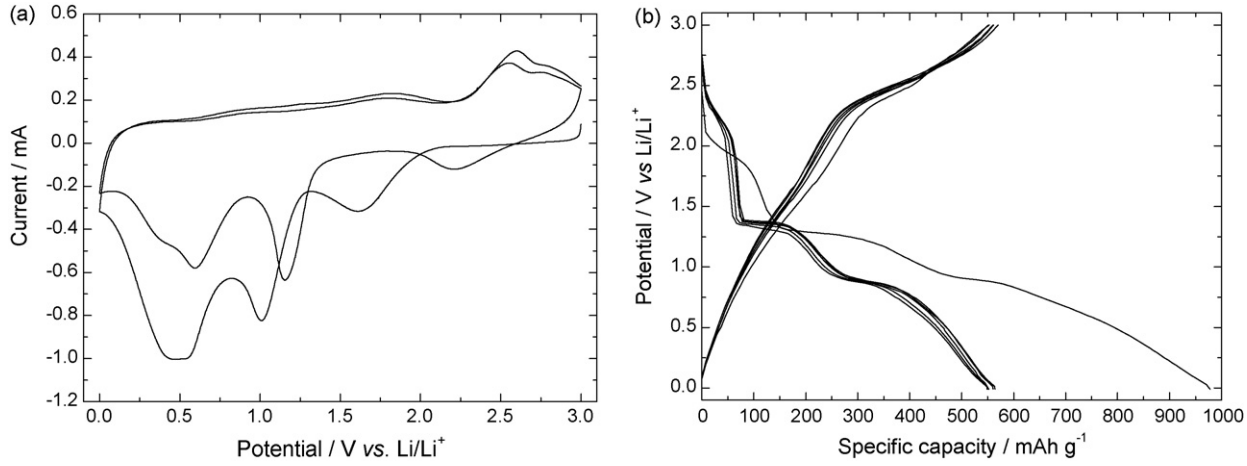

Fig. 5. Cyclic voltammograms (a) and discharge–charge plots (b) of the CuO electrode. Scan rate: 0.5 mV s^{-1}.

capacity at 520 mAh g^{-1} even cycling for 50 cycles, indicating good capacity retention.

Another excellent property associated with this CuO electrode is its high rate capability, and the charge capacity as a function of cycling number at different rates is illustrated in Fig. 7. At first, the cell was cycled at 0.3*C* for 5 cycles, and then the rate was increased to 3*C*. A charge capacity of around 566 mAh g^{-1} is obtained at a rate of 0.3*C* after 5 cycles; this value decreases to 540 mAh g^{-1} at 0.6*C*, 450 mAh g^{-1} at 1*C*, 410 mAh g^{-1} at 1.5*C*, 370 mAh g^{-1} at 2*C*, and finally

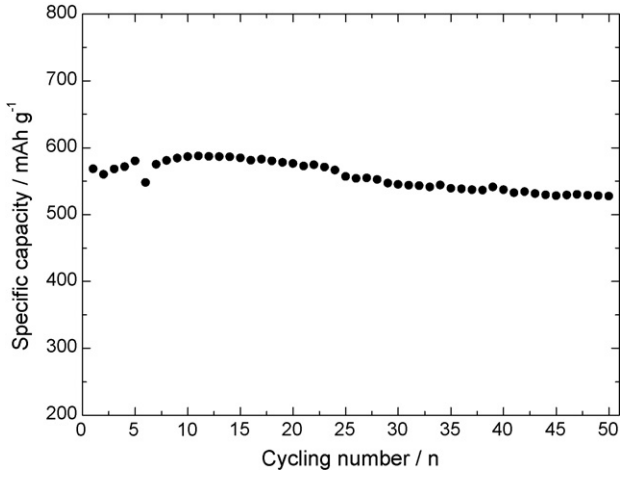

Fig. 6. Specific capacity of the CuO electrode as a function of cycling numbers.

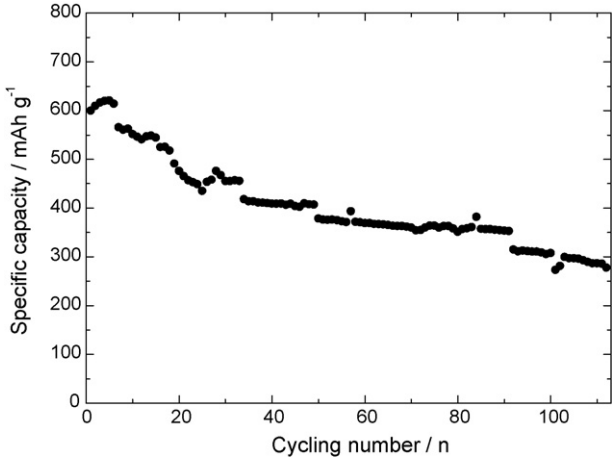

Fig. 7. Charge capacity of the CuO electrode at different discharge–charge rates.

300 mAh g^{-1} at 3*C*. This result indicates the CuO electrode exhibits good rate performance in lithium ion batteries.

It is well known that the rate-limiting step of lithium ion batteries is mainly determined by the solid-state diffusion of lithium ions in active materials [32,33]. A practical pathway to improve the rate performance of lithium ion batteries is to reduce the diffusion path of active materials and to increase the electrode/electrolyte interface area [34]. As a result, high rate capability of the CuO electrode results from the feature nanostructure of CuO film, i.e. CuO fibers at nanoscale shorten the transport path for lithium ions, and network-like architectures increase the electrode/electrolyte contact area. However, the rate performance of electrode is also affected by charge-transfer reaction at the active materials/collector surface. Another reason responsible for the high rate capability is better electrical contact between the active CuO and copper collector. In this case, the CuO nanofibers are directly constructed on the copper surface and they exhibit interwoven architectures. As a result, the electronic kinetics of the CuO electrode is faster than that of the electrode fabricated from polymer binder and conducting agent. This result demonstrates that the network-like CuO film can provide efficient transport for both electrons and lithium ions among the Cu/CuO/electrolytes interfaces.

4. Conclusion

In summary, CuO nanofibers with network-like architectures were fabricated on copper substrate through a simple solution-immersion step and subsequent heat treatment. The resulted CuO film exhibits not only a capacity of 560 mAhg^{-1}, but also high rate capability and good cyclability as negative electrode in lithium ion batteries. One advantage of this method is that it avoids the use of polymer binder and conducting agent that necessary to the conventional electrode-preparation process. We think that the present findings create a new and attractive negative electrode with good electrochemical performance for lithium ion batteries, which is simple, environmental friendly, easy control, and low cost. The result of this study also opens the possibility for the application of well-ordered nanostructures of other transition metal oxides in the field of lithium ion batteries. Studies on the optimization of preparation conditions, the control of surface morphology and its effect on the CuO electrochemical performance are currently underway.

References

[1] Q.M. Pan, H.B. Wang, Y.H. Jiang, J. Mater. Chem. 17 (2007) 329.
[2] L.J. Fu, H. Liu, C. Li, Y.P. Wu, E. Rahm, R. Holze, H.Q. Wu, Solid State Sci. 8 (2006) 113.
[3] Q.M. Pan, H.B. Wang, Y.H. Jiang, Electrochem. Commun., doi:10.1016/j.elecom.2006.11.013, in press.
[4] J.M. Tarascon, M. Armand, Nature 414 (2001) 359.
[5] K.T. Lee, J.C. Lytle, N.S. Ergang, S.M. Oh, A. Stein, Adv. Funct. Mater. 15 (2005) 547.
[6] Y.S. Hu, L. Kienle, Y.G. Guo, J. Maier, Adv. Mater. 18 (2006) 1421.
[7] J. Maier, Nat. Mater. 4 (2005) 805.
[8] R. Dedryvere, S. Laruelle, S. Grugeon, P. Poizot, D. Gonbeau, J.M. Tarascon, Chem. Mater. 16 (2004) 1056.
[9] P. Poizot, S. Laruelle, S. Grugeon, L. Dupont, J.M. Tarascon, Nature 407 (2000) 496.
[10] X.P. Gao, J.L. Bao, G.L. Pan, H.Y. Zhu, P.X. Huang, F. Wu, D.Y. Song, J. Phys. Chem. B 108 (2004) 5547.
[11] S.S. Zhang, K. Xu, T.R. Jow, J. Power Sources 138 (2004) 226.
[12] K.A. Striebel, A. Sierra, J. Shim, C.W. Wang, A.M. Sastry, J. Power Sources 134 (2004) 241.
[13] J. Shim, K.A. Striebel, J. Power Sources 130 (2004) 247.
[14] W. Ho Ghim, A.S.W. Wong, A.T.S. Wee, M.E. Welland, Nano Lett. 4 (2004) 2023.
[15] X.C. Jiang, T. Herricks, Y.N. Xia, Nano Lett. 12 (2002) 1333.
[16] W.X. Zhang, X.G. Wen, S.H. Yang, Inorg. Chem. 42 (2003) 5005.
[17] X.G. Wen, W.X. Zhang, S.H. Yang, Nano Lett. 2 (2002) 1397.
[18] X.F. Wu, G.Q. Shi, J. Phys. Chem. B 110 (2006) 11247.
[19] D.W. Zhang, C.H. Chen, J. Zhang, F. Ren, Chem. Mater. 17 (2005) 5242.
[20] C.T. Hsieh, J.M. Chen, H.H. Lin, H.C. Shih, Appl. Phys. Lett. 83 (2003) 3383.
[21] X.G. Wen, Y.T. Xie, C.L. Choi, K.C. Wan, X.Y. Li, S.H. Yang, Langmuir 21 (2005) 4729.
[22] X.F. Wu, H. Bai, J.X. Zhang, F.E. Chen, G.Q. Shi, J. Phys. Chem. B 109 (2005) 22836.
[23] H. Hou, Y. Xie, Q. Li, Cryst. Growth Des. 5 (2005) 201.
[24] P. Podhajecky, J. Power Sources 14 (1985) 269.
[25] P. Podhajecky, Electrochim. Acta 35 (1990) 245.
[26] G.F. Zou, H. Li, D.W. Zhang, K. Xiong, C. Dong, Y.T. Qian, J. Phys. Chem. B 110 (2006) 1632.
[27] P. Novak, Electrochim. Acta 30 (1985) 1687.
[28] D. Larcher, C. Masquelier, D. Bonnin, Y. Chabre, V. Masson, J.B. Leriche, J.M. Tarascona, J. Electrochem. Soc. 150 (2003) A133.
[29] T. Doi, A. Fukuda, Y. Iriyama, T. Abe, Z. Ogumi, K. Nakagawa, T. Ando, Electrochem. Commun. 7 (2005) 10.
[30] G.T. Wu, C.S. Wang, X.B. Zhang, H.S. Yang, Z.F. Qi, W.Z. Li, J. Power Sources 75 (1998) 175.
[31] P. Novak, B. Klapste, P. Podhajecky, J. Power Sources 15 (1985) 101.
[32] M.D. Levi, D. Aurbach, J. Phys. Chem. B 101 (1997) 4661.
[33] H.Y. Wang, T. Abe, S.H. Maruyama, Y. Iriyama, Z. Ogumi, K. Yoshikawa, Adv. Mater. 17 (2005) 2857.
[34] C.J. Curtis, J. Wang, D.L. Schulz, J. Electrochem. Soc. 151 (2004) A590.